










Intermediate-mass Black Holes from High Massive-star Binary Fractions in Young Star Clusters

Elena González^{1,2}, Kyle Kremer^{2,3,4} , Sourav Chatterjee⁵ , Giacomo Fragione² , Carl L. Rodriguez⁶ ,
Newlin C. Weatherford² , Claire S. Ye² , and Frederic A. Rasio² 

¹ Department of Astronomy, University of Florida, Gainesville, FL 32611, USA; elenagonzalez@ufl.edu

² Center for Interdisciplinary Exploration & Research in Astrophysics (CIERA) and Department of Physics & Astronomy, Northwestern University, Evanston, IL 60208, USA

³ TAPIR, California Institute of Technology, Pasadena, CA 91125, USA

⁴ The Observatories of the Carnegie Institution for Science, Pasadena, CA 91101, USA

⁵ Tata Institute of Fundamental Research, Homi Bhabha Road, Navy Nagar, Colaba, Mumbai 400005, India

⁶ McWilliams Center for Cosmology, Department of Physics, Carnegie Mellon University, Pittsburgh, PA 15213, USA

Received 2020 December 18; revised 2021 January 20; accepted 2021 January 21; published 2021 February 19

Abstract

Black holes formed in dense star clusters, where dynamical interactions are frequent, may have fundamentally different properties than those formed through isolated stellar evolution. Theoretical models for single-star evolution predict a gap in the black hole mass spectrum from roughly 40–120 M_{\odot} caused by (pulsational) pair-instability supernovae. Motivated by the recent LIGO/Virgo event GW190521, we investigate whether black holes with masses within or in excess of this “upper-mass gap” can be formed dynamically in young star clusters through strong interactions of massive stars in binaries. We perform a set of N -body simulations using the CMC cluster-dynamics code to study the effects of the high-mass binary fraction on the formation and collision histories of the most massive stars and their remnants. We find that typical young star clusters with low metallicities and high binary fractions in massive stars can form several black holes in the upper-mass gap and often form at least one intermediate-mass black hole. These results provide strong evidence that dynamical interactions in young star clusters naturally lead to the formation of more massive black hole remnants.

Unified Astronomy Thesaurus concepts: [Young star clusters \(1833\)](#); [Intermediate-mass black holes \(816\)](#); [Stellar mergers \(2157\)](#); [Binary stars \(154\)](#); [N-body simulations \(1083\)](#)

1. Introduction

Since the first binary black hole (BBH) detection by the Laser Interferometer Gravitational-Wave Observatory (LIGO)/Virgo in 2015 (Abbott et al. 2016), the field of gravitational wave (GW) astrophysics has taken off. The recent release of the second Gravitational Wave Transient Catalog by LIGO/Virgo (Abbott et al. 2020b) has increased significantly the number of known GW events, enabling new and powerful constraints on cosmology, fundamental physics, and various aspects of stellar astrophysics (e.g., The LIGO Scientific Collaboration et al. 2020a, 2020b). In particular, the ability to describe the population properties of the compact objects involved in the mergers has helped both confirm models for massive star evolution and test the limits of our theories (e.g., The LIGO Scientific Collaboration et al. 2020c).

Key evolutionary stages of massive stars expected to leave a strong imprint on the shape of the black hole (BH) mass spectrum are pair-instability supernovae (PISNe) and pulsational pair-instability supernovae (PPISNe). These occur when evolved stars with core masses between roughly 45 and 135 M_{\odot} experience at the onset of carbon burning a decrease in radiation pressure and core contraction, associated with electron–positron pair production (e.g., Barkat et al. 1967). Consequently, depending on the final stellar core mass, a series of runaway thermonuclear explosions can either significantly enhance mass loss (PPISN) or completely destroy the star, leaving behind no remnant (PISN; Fowler & Hoyle 1964; Ober et al. 1983; Bond et al. 1984; Heger & Woosley 2002; Woosley et al. 2007; Belczynski et al. 2016; Woosley 2017, 2019). Recent calculations show that PISNe and PPISNe can prevent

the formation of BHs with masses in the range ≈ 40 –120 M_{\odot} , with the exact boundaries remaining somewhat uncertain (e.g., Spera & Mapelli 2017; Woosley 2017; Limongi & Chieffi 2018; Takahashi et al. 2018; Farmer et al. 2019; Marchant et al. 2019; Stevenson et al. 2019; Belczynski et al. 2020; Costa et al. 2020; Mapelli et al. 2020; Renzo et al. 2020).

GW190521, a BBH merger with component masses of about 66 M_{\odot} and 85 M_{\odot} (Abbott et al. 2020a), revealed for the first time evidence of BHs with masses in the so-called “upper-mass gap” expected from pair instabilities. In total, the first half of LIGO/Virgo’s third observing run revealed eight BBH mergers with at least one component with mass in excess of 45 M_{\odot} , five of which have at least one component in excess of 60 M_{\odot} . The direct detections of these massive BHs spark a number of questions concerning the stellar BH mass spectrum and prompts a detailed examination of our understanding of stellar evolution models.

A number of recent analyses have examined ways that BHs with masses residing in the upper-mass gap may form. Possibilities include hierarchical mergers of lower-mass BHs (e.g., Miller & Hamilton 2002; McKernan et al. 2012; Rodriguez et al. 2018, 2019; Antonini et al. 2019; Gerosa & Berti 2019; Fragione & Silk 2020; Fragione et al. 2020), primordial BHs formed through collapse of gravitational instabilities in the early universe (e.g., Loeb & Rasio 1994; Carr et al. 2016), Population III stars (e.g., Madau & Rees 2001; Bromm & Larson 2004), growth through gas accretion in star-forming environments (e.g., Roupas & Kazanas 2019), and stellar mergers in dense star clusters (e.g., Di Carlo et al. 2019; Banerjee 2020; Banerjee et al. 2020; Kremer et al. 2020a;

Rizzuto et al. 2020). In the latter case, a merger between a main-sequence star and an evolved star leads to the formation of a helium core that could survive the supernova explosion and result in a BH more massive than could ever be formed through single-star evolution (Spera et al. 2019). This is closely related to the collisional runaway process that has long been associated with the formation of intermediate-mass black holes (IMBHs), with masses in the range $\approx 10^2\text{--}10^5 M_\odot$ (e.g., Zwart et al. 2004; Gürkan et al. 2006; Giersz et al. 2015; Mapelli 2016). The existence of IMBHs in dense star clusters has been debated for decades, with possible evidence coming in the form of X-ray/radio sources and dynamical measurements (for a recent review, see Greene et al. 2020). The roughly $150 M_\odot$ BH observed as the merger product of GW190521 provides the first *direct* evidence of IMBH formation. If indeed GW190521 was dynamically formed in a star cluster, it would be the strongest evidence yet that IMBHs, and massive BHs more broadly, can form in dense stellar environments.

In the dynamical evolution of young star clusters, one of the most crucial parameters pertaining to massive stars is the primordial binary fraction. For stars in the Galactic field, observations suggest that nearly 100% of O- and B-type stars reside in binaries at birth (e.g., Sana et al. 2012; Moe & Di Stefano 2017). The binary fraction (both primordial and at late times) in stellar clusters is less well constrained. Many old globular clusters (GCs) are observed to have low binary fractions ($\lesssim 10\%$) at present, even though their primordial binary fractions at birth may have been higher (e.g., Ivanova et al. 2005; Milone et al. 2012).

On the other hand, young massive clusters (YMCs) in the local universe have measured binary fractions comparable to those seen in the field (e.g., Sana et al. 2009). Progenitors of today’s GCs are widely thought to have had properties similar to present-day YMCs, but with much lower metallicities (e.g., Chatterjee et al. 2010, 2013). Although a direct connection between YMCs and GCs remains elusive due to a lack of observed intermediate clusters (e.g., Portegies Zwart et al. 2010), the high observed binary fractions in YMCs suggest that a high binary fraction for massive stars may be present in all star clusters at birth.

The importance of stellar binaries for star cluster dynamics has been understood for decades, with binaries expected to serve as an important dynamical energy source and to slow down gravothermal contraction (e.g., Heggie & Hut 2003; Chatterjee et al. 2013, 2010). Binaries also play a significant role in producing high rates of both stellar collisions (e.g., Fregeau & Rasio 2007) and BH mergers (e.g., Chatterjee et al. 2017).

In this study, we explore the effect of high-mass binary fraction upon the short-term evolution of dense star clusters with a specific focus on stellar collisions and the formation of massive BHs that may lie within or above the pair-instability mass gap.

This Letter is organized as follows. We describe our methods for modeling clusters in Section 2. In Section 3 we present our results from numerical simulations, including the formation paths for the most massive BHs. We also study the effects of the primordial high-mass binary fraction and the initial virial radius of clusters on BH formation. Finally, we discuss our results and conclude in Section 4.

2. Models of Cluster Evolution

We perform numerical simulations using CMC (for Cluster Monte Carlo), a Hénon-type Monte Carlo code that models the evolution of stellar clusters (Pattabiraman et al. 2013; Kremer et al. 2020b). This code incorporates prescriptions for various physical processes including two-body relaxation (Joshi et al. 2000), stellar/binary evolution using the population synthesis code COSMIC (Breivik et al. 2020), direct integration of small- N strong encounters using Fewbody (Fregeau & Rasio 2007), and stellar collisions (Fregeau & Rasio 2007). See Section 2.1 of Kremer et al. (2020b) for a summary of CMC and Section 2 of Kremer et al. (2020a) for a detailed discussion of our treatment of collision cross sections, properties and evolution of collision products, and compact object formation for this set of simulations. A standard $\alpha\gamma$ model is adopted for common envelope (CE) evolution (Hurley et al. 2002). The CE efficiency constant is $\alpha = 1.0$ and the binding-energy is set according to previous studies (see Section 3.2 in Breivik et al. 2020 for a recent overview of CE prescriptions in COSMIC).

The present study is based on the set of models listed in Table 1. All models consist of 8×10^5 objects, corresponding to an initial total cluster mass of $4.7 \times 10^5 M_\odot$. The metallicity is set to 0.002 ($0.1 Z_\odot$) and the initial conditions are King models with concentration parameter $W_0 = 5$. Stellar masses (primary masses for binaries) are sampled from a Kroupa (2001) initial mass function in the range $0.08\text{--}150 M_\odot$. To increase the robustness of our results, we run multiple realizations of each set of initial parameters with different random seeds.

We vary in our models the initial virial radius, r_v , and the high-mass binary fraction, $f_{b,\text{high}}$, defined as the fraction of primaries with mass above $15 M_\odot$ that have a companion at the time of cluster formation. The simulations performed include values for r_v of 1, 1.2 and 1.5 pc and $f_{b,\text{high}}$ of 0% and 100%. For all models, the low-mass ($< 15 M_\odot$) binary fraction is fixed at 5%. For low-mass binaries, primary masses are drawn randomly from our IMF, secondary masses are drawn assuming a flat mass ratio distribution in the range $[0.1, 1]$, and initial orbital periods are drawn from a log-uniform distribution $dn/d \log P \propto P$. For the secondaries of the massive stars ($> 15 M_\odot$), a flat mass ratio distribution in the range $[0.6, 1]$ is assumed and initial orbital periods are drawn from the distribution $dn/d \log P \propto P^{-0.55}$ (e.g., Sana et al. 2012).

For all binaries, the initial orbital periods are drawn from near contact to the hard-soft boundary and eccentricities are assumed to be thermal. The simulations are limited to 30 Myr as we focus on massive star evolution and BH formation.

In this Letter we define “pair-instability gap” (or “upper-mass gap”) BHs to be those with masses in the range $40.5\text{--}120 M_\odot$, as determined by our assumed prescriptions for pair-instability physics (for details, see Belczynski et al. 2016; Kremer et al. 2020a). Although the pair-instability gap range considered is roughly consistent with that inferred from the latest LIGO/Virgo observations (The LIGO Scientific Collaboration et al. 2020c), we note that the exact boundaries of this gap are uncertain and depend upon various assumptions regarding massive star physics (e.g., Spera & Mapelli 2017; Woosley 2017; Limongi & Chieffi 2018; Takahashi et al. 2018; Farmer et al. 2019; Marchant et al. 2019; Stevenson et al. 2019; Belczynski et al. 2020; Costa et al. 2020; Mapelli et al. 2020; Renzo et al. 2020). However, we stress that changes to the

Table 1
List of Cluster Models

Model	r_v (pc)	$f_{b,high}$	N_{BH} (total)	N_{BH} (dyn coll.)	N_{BH} (bin coal.)	N_{PIgap}	N_{IMBH}	$M_{BH,max}$ (M_\odot)	Massive Star Mergers	
									(dyn coll.)	(bin coal.)
1a	1	0	2259	240	0	0	0	40.50	356	0
1b	1	0	2257	235	0	0	0	40.50	390	0
1c	1	0	2254	232	0	1	0	75.68	364	0
1d	1	0	2259	241	0	0	0	40.50	390	0
2a	1	1	2883	233	760	3	2	598.28	656	792
2b	1	1	2342	154	155	7	2	230.29	409	170
2c	1	1	2318	171	164	4	1	239.80	489	178
2d	1	1	2185	158	160	7	0	92.05	411	165
2e	1	1	3223	240	155	7	2	443.32	664	176
2f	1	1	2588	175	167	5	2	279.24	474	188
2g	1	1	2180	159	162	3	0	85.53	435	172
2h	1	1	2170	193	156	3	0	82.45	722	167
2i	1	1	2493	174	159	3	2	252.78	511	177
2j	1	1	2169	177	158	2	0	90.97	476	166
2k	1	1	3249	239	171	11	2	468.84	607	189
2l	1	1	2167	165	150	8	1	143.30	461	162
2m	1	1	2214	139	146	4	1	203.54	360	165
2n	1	1	2152	152	155	4	0	103.67	432	167
2o	1	1	2185	146	149	2	0	85.93	412	168
2p	1	1	2165	152	161	1	1	154.85	443	174
2q	1	1	2329	146	161	3	2	228.79	436	177
2r	1	1	2185	157	151	2	0	98.64	377	157
2s	1	1	2739	166	151	0	1	303.11	516	174
2t	1	1	2192	138	160	7	0	99.20	345	164
2u	1	1	2175	154	150	4	0	96.43	439	172
2v	1	1	2172	121	154	2	0	90.38	361	165
2w	1	1	2186	165	150	6	1	145.55	451	169
2x	1	1	2289	187	152	4	2	226.72	454	172
3a	1.2	1	2239	101	211	3	0	93.59	201	226
3b	1.2	1	2199	89	220	2	0	78.72	151	231
3c	1.2	1	2215	84	213	1	0	49.41	161	226
3d	1.2	1	2221	94	210	2	0	88.46	177	227
3e	1.2	1	2290	87	214	2	1	217.44	185	228
3f	1.2	1	2183	84	216	1	0	82.63	163	226
3g	1.2	1	2247	78	219	1	0	71.19	148	227
3h	1.2	1	2210	103	216	1	0	57.59	189	224
3i	1.2	1	2230	105	217	4	0	99.08	187	227
4a	1.5	1	2335	45	621	2	1	132.66	59	625
4b	1.5	1	2321	40	623	0	0	40.50	68	631
4c	1.5	1	2357	38	621	0	0	40.50	54	627
4d	1.5	1	2340	54	613	0	0	40.50	75	624
4e	1.5	1	2356	43	619	1	0	81.27	68	626

Note. List of all cluster models included in this study. In column 2 we indicate the initial virial radius in units of parsecs. Column 3 lists the primordial high-mass binary fraction for the models. Column 4 shows the total number of black holes formed. Columns 5–6 show the number of black holes in the first two formation paths listed in Section 3.1. Columns 7–8 indicate the number of black holes formed with masses in the pair-instability gap ($40.5\text{--}120 M_\odot$) and number of IMBHs, respectively. Column 9 lists the most massive black hole formed in solar masses. In columns 10 and 11 we show the total number of massive star collisions and massive binary coalescences where at least one mass component is massive ($M > 15 M_\odot$) and all components are either giants or main sequence stars.

assumed boundaries of the pair-instability gap are unlikely to affect our results. Here we use the term “IMBH” to refer specifically to BHs with $M > 120 M_\odot$, beyond our assumed upper boundary for the pair-instability gap. We use “massive BH” as a general term to refer to any BH with mass greater than $40.5 M_\odot$.

3. Results

3.1. Formation Channels

We distinguish formation channels based on the BH progenitor’s primary method of growth. Illustrated in the two left-most panels of Figure 1 are characteristic examples of the two formation paths that we have identified in our simulations.

- (1) *Direct physical collisions*: the direct physical collision scenario occurs when most of the BH progenitor mass is accumulated via dynamical interactions (either single–

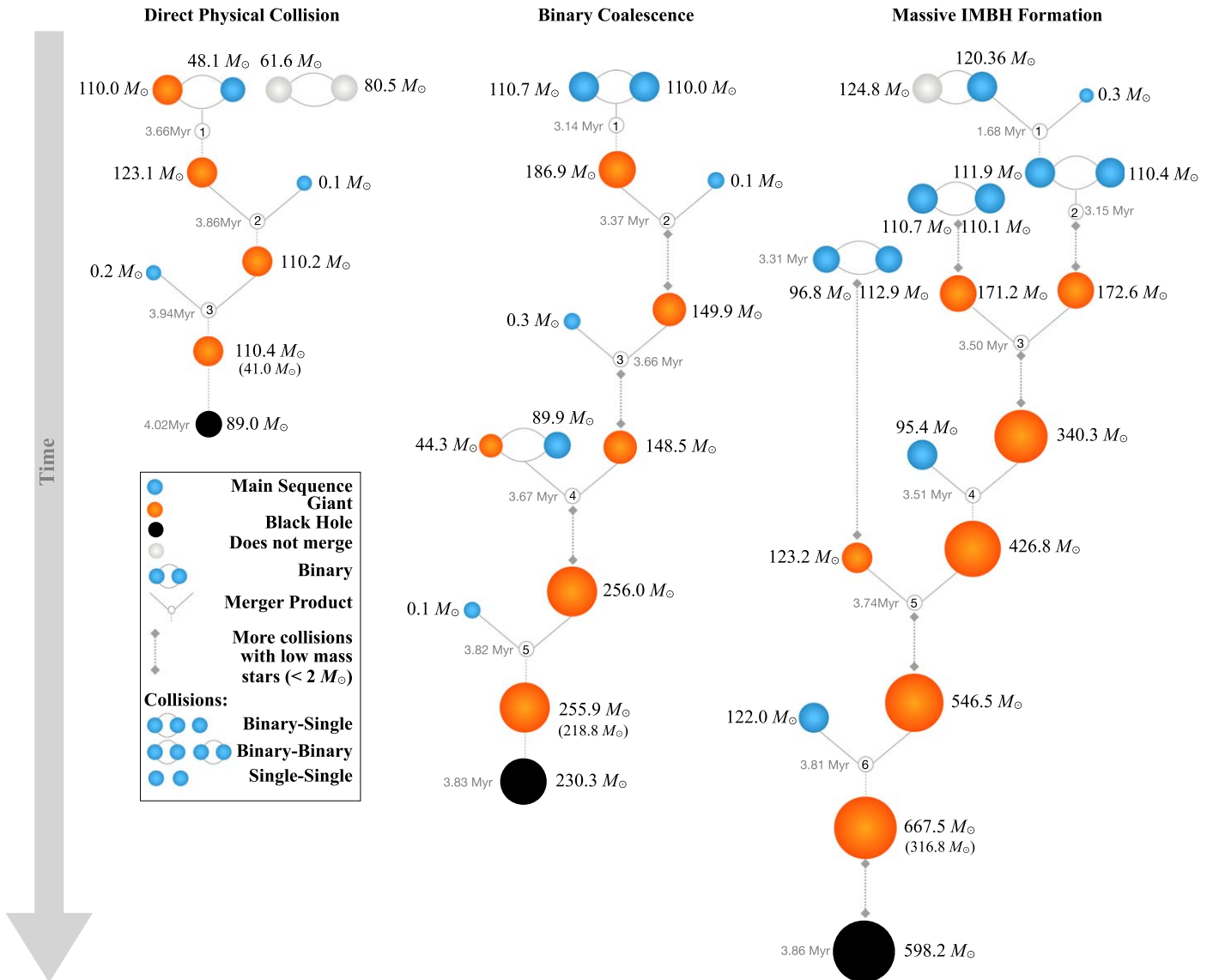


Figure 1. The first two panels from the left illustrate the different formation paths described in Section 3.1. In the direct physical collision scenario, the dominant process by which the principal object increases in mass is through physical collisions, as is shown by the initial binary–binary interaction that leads to the merger of two stars. In contrast, in the middle, for the formation path labeled binary coalescence, the main increase in mass comes from binary coalescence. The right-most column illustrates the collision history of the most massive IMBH formed in our simulations. We show the total mass of each object involved in the dynamical interactions. We show in parentheses the core mass just before BH formation.

single or binary-mediated) that lead to stellar collisions. In the example shown in the left-most panel of Figure 1, an initial binary–binary encounter leads to a collision and merger of one of the primordial binaries.

- (2) *Binary coalescence*: the second formation channel occurs when most of the mass growth comes from binary stellar evolution processes, in particular binary coalescence resulting from common envelope episodes. In this case, any subsequent dynamical collisions contribute less mass in total than the initial binary coalescence. The middle panel in Figure 1 shows an example of a binary coalescence formation path.

We identify an additional formation path which is a subset of the “direct physical collisions” channel. In this scenario, which is illustrated in the right panel of Figure 1, the stars involved in the key dynamical collisions (e.g., collisions 3 and 5 in the

right panel of Figure 1) are themselves products of primordial binary coalescences.

Although this “hybrid” channel is only observed in the formation history of three BHs in our models, it is notable because it highlights the interdependence of dynamics and binary evolution. Furthermore, it is the formation path of the most massive IMBH that we observe in this study (roughly $600 M_{\odot}$).

Of all BHs formed in our models (fourth column of Table 1), 6.2% are formed through the direct physical collision path (column five) and 9.6% are labeled as binary coalescence (column six). The rest of the BHs are formed through standard isolated stellar evolution (i.e., experience no dynamical/binary evolution before BH formation). For the massive BHs specifically, 95.9% and 4.1% fall into the direct collision and binary coalescence channels, respectively. For the massive BHs that are classified under the direct collisions path, 100% feature at least one binary-mediated dynamical collision prior to

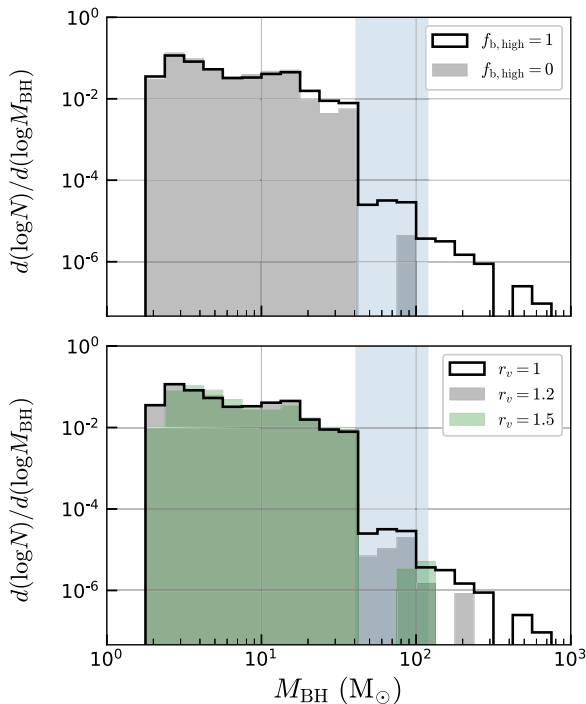


Figure 2. Normalized BH mass distribution for the models listed in Table 1. The top panel shows the BH mass spectrum comparison between the two models with high-mass binary fraction 0 and 1 and a virial radius of 1 pc. The bottom panel shows the BH spectrum for the different values of r_v (we use the initial virial radius of the assumed King model to determine the initial cluster density) and a fixed high-mass binary fraction of 1. The shaded blue region indicates the “upper-mass gap.”

formation, indicating the presence of primordial binaries plays a key role in massive BH formation. This is markedly different from the results of Kremer et al. (2020a) where, in the absence of primordial stellar binaries, mass growth through binary-evolution-mediated processes never occurred. The pronounced increase in the number of massive BHs in the presence of primordial binaries is the principal result of this study.

3.2. Primordial High-mass Binary Fraction

To isolate the effect of $f_{b,\text{high}}$, the top panel of Figure 2 compares the BH mass distributions for the models with $f_{b,\text{high}} = 0, 1$ and fixed $r_v = 1$ pc. The blue background marks the assumed boundaries for the pair-instability mass gap. The most notable difference between the two histograms is the presence of the extended tail of massive BHs ($M > 40.5 M_\odot$) in the model with $f_{b,\text{high}} = 1$ that is not present in the $f_{b,\text{high}} = 0$ case. As shown in Table 1, models with $f_{b,\text{high}} = 1$ (and $r_v = 1$ pc) produce, on average, four BHs with masses in the range $40.5\text{--}120 M_\odot$ (our assumed pair-instability gap) and one BH with mass in excess of $120 M_\odot$. In contrast, for the models with $f_{b,\text{high}} = 0$, we identify only one pair-instability gap BH and zero BHs with masses larger than $120 M_\odot$.⁷ It is clear from these results that the high-mass binary fraction makes a strong imprint on the BH mass distribution.

3.3. Virial Radii

In the bottom panel of Figure 2, we plot the BH mass distributions for all of the r_v models listed in Table 1 and fixed

$f_{b,\text{high}} = 1$. It is clear that more compact clusters (smaller r_v) form a higher number of massive BHs, both within and above the mass gap. For example, in the models with $r_v = 1$ pc we see approximately 10 times more massive star collisions than in the models with $r_v = 1.5$ pc. This is to be expected as a denser environment will increase the rate of dynamical collisions of massive stars (see column 10 in Table 1). The drastic change in mass of the heaviest BH formed between the models with virial radius 1 and 1.5 pc indicates that small changes in the density of a cluster can greatly influence the BH mass spectrum. As detailed in column 9 in Table 1, the most massive BH formed in the model with $r_v = 1$ pc is approximately $600 M_\odot$ while the model with $r_v = 1.5$ pc has a maximum BH mass of $132 M_\odot$. Meanwhile, we observe a clear decrease in the rate of massive BH formation in models with $r_v > 1.2$ pc.

3.4. The Role of High-mass Binaries in BH Formation

Here we examine the different realizations of model 2 in Table 1 ($r_v = 1$ pc and $f_{b,\text{high}} = 1$). As shown in Table 1, there is a difference in the number of BHs formed among the runs, with some producing as few as 2300 BHs and other as many as 3200 BHs. Enhanced BH production occurs in the runs that form the most massive IMBHs, such as models 2a, 2e and 2k, which produce IMBHs ranging from roughly $400\text{--}600 M_\odot$. The most massive IMBH in these models forms at ~ 3 Myr, while the increase in BH formation rate occurs between 7 and 15 Myr.

This excess in BH number can be partially explained by an increase in binary interaction rates in these models. Specifically, model 2a has a higher number of binary mergers involving stars with zero-age main sequence (ZAMS) masses between 10 and $25 M_\odot$ that would not have otherwise been BH progenitors (at $0.1 Z_\odot$, the minimum ZAMS mass that will form a BH is roughly $20 M_\odot$). However, these merger products do evolve into BHs with masses roughly in the range of $M_{\text{BH}} \approx 5\text{--}15 M_\odot$. For models 2e and 2k, the higher number of BHs can be partially attributed to mass transfer in a binary increasing the mass of one of the components past the threshold of BH formation. Naturally, some of these differences are clearly due to stochastic fluctuations in the initial evolution of the model, leading to divergent paths in the dynamical evolution of the system. The main takeaway is that binary evolution processes, coupled with dynamics, can greatly influence BH growth. We leave a detailed study of the extent to which binary evolution processes affect the long-term cluster evolution and dynamics for a future study.

It is important to note that many (roughly 55%) of these “excess” BHs formed with masses less than $15 M_\odot$ are ejected promptly from their host cluster through natal kicks. Low-mass BHs are expected to form with less mass fallback and thus receive larger natal kicks (e.g., Fryer et al. 2012). Thus, this excess of BHs formed is unlikely to have a significant effect on the long-term cluster dynamics.

4. Discussion and Conclusions

Our results show that high binary fractions for massive stars lead to an increase in binary-mediated dynamical interactions, which in turn have an important effect on massive BH formation. We have demonstrated that increasing the high-mass binary fraction, consistent with observations, while keeping all other cluster parameters (e.g., cluster masses, virial radii, metallicity) fixed at the values used in Kremer et al. (2020b),

⁷ See Kremer et al. (2020a) for further information on the $f_{b,\text{high}} = 0$ models.

may significantly change the early evolution of YMCs. In particular, high-mass binaries facilitate high rates of massive star collisions (occurring through both dynamical encounters and binary-evolution-driven mergers) that can lead to the formation of massive BHs, both within and above the pair-instability mass gap. With the exception of the high-mass binary fraction, the parameters for the models calculated in this Letter are identical to those in Kremer et al. (2020b), which were shown to lead to present-day properties matching well those of Milky Way GCs. If indeed the majority of high-mass stars have binary companions at birth, massive BH formation may therefore be a common occurrence in the early phases of GC evolution.

As shown in Figure 2, the formation of massive BHs is sensitive to small changes in initial virial radius. This is in agreement with previous works on the topic of IMBH formation that have shown that the onset of a collisional runaway occurs abruptly under small changes to cluster parameters (e.g., Gürkan et al. 2004; Portegies Zwart et al. 2004; Giersz et al. 2015; Mapelli 2016). Indeed, the CMC models presented in Kremer et al. (2020a) exhibited a similar sharp dependence on r_v . However, Kremer et al. (2020a), which assumed zero primordial binaries, found that the onset of collisional runaways occurred at $r_v \lesssim 0.8$ pc, while here the transition occurs at $r_v \approx 1$ pc. Not surprisingly, the presence of primordial binaries increases the collision rate and therefore moves the threshold for collisional runaway to larger cluster sizes. Kremer et al. (2020b) showed that varying r_v from about 0.5–4 pc can explain naturally the full range of GC properties observed at present in the Milky Way. Thus, small changes to the minimum r_v value that lead to collisional runaways may have deep repercussions on the theoretical predictions for the presence of IMBHs in GCs.

In this study, we have focused on the first 30 Myr of cluster evolution to explore the formation of massive BHs. After their formation, these BHs can acquire, retain, and lose close companion stars and compact objects through few-body interactions (e.g., Sigurdsson & Hernquist 1993; Morscher et al. 2015; MacLeod et al. 2016). If the mass of one of the BHs is high enough, a cusp of objects can efficiently grow, affecting the innermost regions of the host cluster (e.g., Baumgardt et al. 2005; Heggie et al. 2007; Lützgendorf et al. 2013). Some of the closest companions could form hierarchically separated binaries with the massive BHs and persist until they are replaced in few-body encounters (Fragione & Bromberg 2019). Eventually, close interactions with the massive BHs can lead to the tidal disruption of a star or the inspiral and merger of a compact object (e.g., Haster et al. 2016; Fragione et al. 2018a, 2018b). We leave the detailed study of the long-term dynamics of massive BHs to future work.

The recently released data from the first half of LIGO/Virgo’s third observing run provides strong evidence for the formation of BHs with masses in the pair-instability gap (Abbott et al. 2020b; The LIGO Scientific Collaboration et al. 2020c). Thus, the results of this study may have important implications for GW astrophysics. In lieu of integration of the cluster models presented here over the full cluster lifetime ($\gtrsim 10$ Gyr), we perform an order-of-magnitude estimate to

determine the rate of mass-gap BBH mergers. Consider here only those models with $r_v = 1$ pc. If we assume for simplicity that every mass-gap BH in our $f_{b,\text{high}} = 1$ models goes on to undergo one⁸ (dynamically formed) BBH merger within a Hubble time (as discussed in Kremer et al. 2020a, this is a reasonable assumption), we predict, on average, four mass-gap mergers per cluster.

The most massive BHs in a cluster will be the first to mass-segregate to the center, dynamically form binaries, and merge (e.g., Morscher et al. 2015; Kremer et al. 2020b). Thus, as a crude approximation, we can assume that these BHs merge promptly (with negligible delay time). We can then estimate the volumetric rate of mass-gap mergers at redshift z as

$$\Gamma(z) \approx \frac{N_{\text{gap}}}{M_{\text{cl}}} \rho_{\text{SF}}(z) f_{\text{SF}} \quad (1)$$

where N_{gap} is the average number of pair-instability gap BHs formed per cluster (from our models, we find $N_{\text{gap}} \approx 4$; again, we assume these also go on to undergo one BBH merger), $M_{\text{cl}} = 4.7 \times 10^5 M_{\odot}$ (the initial cluster mass assumed for our models), and $\rho_{\text{SF}}(z)$ is the cosmological density of the star formation rate at redshift z . At $z = 1$, when metallicities of $0.1Z_{\odot}$ (as assumed for the models in this study) are relevant, ρ_{SF} has a value of roughly $0.1 M_{\odot} \text{ yr}^{-1} \text{ Mpc}^{-3}$ (e.g., Hopkins & Beacom 2006). The (highly uncertain) factor f_{SF} is the fraction of the star formation assumed to occur in star clusters that may yield massive BH mergers. Taking f_{SF} as a free parameter for now, we estimate a mass-gap merger rate of roughly $f_{\text{SF}} \times 100 \text{ Gpc}^{-3} \text{ yr}^{-1}$ at $z \approx 1$ from young massive clusters. In contrast, for our models with $f_{b,\text{high}} = 0$, we find on average 0.2 mass-gap BHs per cluster, which translates to a mass-gap merger rate of roughly $f_{\text{SF}} \times 0.5 \text{ Gpc}^{-3} \text{ yr}^{-1}$ at $z \approx 1$.

Observations suggest that the majority of stars form in stellar clusters or associations (e.g., Lada & Lada 2003) covering a wide mass range. In this study, we have modeled young clusters more representative of the high-mass tail of the cluster mass function, which is expected to scale as M^{-2} (Lada & Lada 2003). It is not clear a priori that the results from our models extend to lower cluster masses $\lesssim 10^5 M_{\odot}$, which dominate the cluster mass function by number. However, recent work by Di Carlo et al. (2019) has shown that massive BHs within or above the pair-instability gap may form through stellar collisions and merge with other BHs in young clusters with masses as low as $10^3 M_{\odot}$. As a simple estimate, we can take $10^3 M_{\odot}$ as the minimum cluster mass yielding massive BH formation and merger. Assuming $10^2 M_{\odot}$ as the minimum value for a cluster/association mass function covering the entire SFR (Lada & Lada 2003), we can then estimate f_{SF} as

$$f_{\text{SF}} \approx \frac{\int_{10^3}^{10^6} M^{-2} dM}{\int_{10^2}^{10^6} M^{-2} dM} \approx 0.1, \quad (2)$$

suggesting a merger rate of massive BHs of roughly $10 \text{ Gpc}^{-3} \text{ yr}^{-1}$ at $z \approx 1$.








While this crude order-of-magnitude estimate is encouraging, a more systematic analysis will be necessary to make

⁸ In principle, a mass-gap BH could undergo more than one BH merger, if the merger products are retained in the cluster. However, given the large recoil kicks associated with GW emission, this has low probability and can be ignored to first approximation.

detailed predictions and determine their theoretical uncertainties. However, regardless of details, it is clear that the primordial high-mass binary fraction in star clusters could play a key role in the formation of massive BH mergers, easily detectable as GW sources by LIGO/Virgo or future GW detectors.

We are grateful to Mario Spera for key insights during the development of this project and we thank him for a careful reading of the manuscript. We thank the anonymous referee for helpful comments. This work was supported by NSF Grants AST-1757792 and AST-1716762 at Northwestern University. N.W. acknowledges support from the CIERA Riedel Graduate Fellowship as well as the NSF GK-12 Fellowship Program under Grant DGE-0948017. K.K. is supported by an NSF Astronomy and Astrophysics Postdoctoral Fellowship under award AST-2001751. G.F. acknowledges support from a CIERA Fellowship at Northwestern University. Computations were made possible through the resources and staff contributions provided for the Quest high-performance computing facility at Northwestern University. S.C. acknowledges support of the Department of Atomic Energy, Government of India, under project No. 12-R&D-TFR-5.02-0200.

ORCID iDs

Kyle Kremer  <https://orcid.org/0000-0002-4086-3180>
 Sourav Chatterjee  <https://orcid.org/0000-0002-3680-2684>
 Giacomo Fragione  <https://orcid.org/0000-0002-7330-027X>
 Carl L. Rodriguez  <https://orcid.org/0000-0003-4175-8881>
 Newlin C. Weatherford  <https://orcid.org/0000-0002-9660-9085>
 Claire S. Ye  <https://orcid.org/0000-0001-9582-881X>
 Frederic A. Rasio  <https://orcid.org/0000-0002-7132-418X>

References

- Abbott, B. P., Abbott, R., Abbott, T. D., et al. 2016, *PhRvL*, **116**, 061102
 Abbott, R., Abbott, T. D., Abraham, S., et al. 2020a, *PhRvL*, **125**, 101102
 Abbott, R., Abbott, T. D., Abraham, S., et al. 2020b, arXiv:2010.14527
 Antonini, F., Gieles, M., & Gualandris, A. 2019, *MNRAS*, **486**, 5008
 Banerjee, S. 2020, *MNRAS*, **500**, 3002
 Banerjee, S., Belczynski, K., Fryer, C. L., et al. 2020, *A&A*, **639**, A41
 Barkat, Z., Rakavy, G., & Sack, N. 1967, *PhRvL*, **18**, 379
 Baumgardt, H., Makino, J., & Hut, P. 2005, *ApJ*, **620**, 238
 Belczynski, K., Heger, A., Gladysz, W., et al. 2016, *A&A*, **594**, A97
 Belczynski, K., Klencki, J., Fields, C. E., et al. 2020, *A&A*, **636**, A104
 Bond, J. R., Arnett, W. D., & Carr, B. J. 1984, *ApJ*, **280**, 825
 Breivik, K., Coughlin, S., Zevin, M., et al. 2020, *ApJ*, **898**, 71
 Bromm, V., & Larson, R. B. 2004, *ARA&A*, **42**, 79
 Carr, B., Kühnel, F., & Sandstad, M. 2016, *PhRvD*, **94**, 083504
 Chatterjee, S., Fregeau, J. M., Umbreit, S., & Rasio, F. A. 2010, *ApJ*, **719**, 915
 Chatterjee, S., Rodriguez, C. L., & Rasio, F. A. 2017, *ApJ*, **834**, 68
 Chatterjee, S., Umbreit, S., Fregeau, J. M., & Rasio, F. A. 2013, *MNRAS*, **429**, 2881
 Costa, G., Bressan, A., Mapelli, M., et al. 2020, arXiv:2010.02242
 Di Carlo, U. N., Giacobbo, N., Mapelli, M., et al. 2019, *MNRAS*, **487**, 2947
 Farmer, R., Renzo, M., de Mink, S. E., Marchant, P., & Justham, S. 2019, *ApJ*, **887**, 53
 Fowler, W. A., & Hoyle, F. 1964, *ApJS*, **9**, 201
 Fragione, G., & Bromberg, O. 2019, *MNRAS*, **488**, 4370
 Fragione, G., Ginsburg, I., & Kocsis, B. 2018a, *ApJ*, **856**, 92
 Fragione, G., Leigh, N. W. C., Ginsburg, I., & Kocsis, B. 2018b, *ApJ*, **867**, 119
 Fragione, G., Loeb, A., & Rasio, F. A. 2020, *ApJL*, **902**, L26
 Fragione, G., & Silk, J. 2020, *MNRAS*, **498**, 4591
 Fregeau, J. M., & Rasio, F. A. 2007, *ApJ*, **658**, 1047
 Fryer, C. L., Belczynski, K., Wiktorowicz, G., et al. 2012, *ApJ*, **749**, 91
 Gerosa, D., & Berti, E. 2019, *PhRvD*, **100**, 041301
 Giersz, M., Leigh, N., Hypki, A., Lützgendorf, N., & Askar, A. 2015, *MNRAS*, **454**, 3150
 Greene, J. E., Strader, J., & Ho, L. C. 2020, *ARA&A*, **58**, 257
 Gürkan, M. A., Fregeau, J. M., & Rasio, F. A. 2006, *ApJL*, **640**, L39
 Gürkan, M. A., Freitag, M., & Rasio, F. A. 2004, *ApJ*, **604**, 632
 Haster, C.-J., Antonini, F., Kalogera, V., & Mandel, I. 2016, *ApJ*, **832**, 192
 Heger, A., & Woosley, S. E. 2002, *ApJ*, **567**, 532
 Hogg, D., & Hut, P. 2003, *The Gravitational Million-Body Problem: A Multidisciplinary Approach to Star Cluster Dynamics* (Cambridge: Cambridge Univ. Press)
 Hogg, D. C., Hut, P., Mineshige, S., Makino, J., & Baumgardt, H. 2007, *PASJ*, **59**, L11
 Hopkins, A. M., & Beacom, J. F. 2006, *ApJ*, **651**, 142
 Hurley, J. R., Tout, C. A., & Pols, O. R. 2002, *MNRAS*, **329**, 897
 Ivanova, N., Belczynski, K., Fregeau, J. M., & Rasio, F. A. 2005, *MNRAS*, **358**, 572
 Joshi, K. J., Rasio, F. A., & Portegies Zwart, S. 2000, *ApJ*, **540**, 969
 Kremer, K., Spera, M., Becker, D., et al. 2020a, arXiv:2006.10771
 Kremer, K., Ye, C. S., Rui, N. Z., et al. 2020b, *ApJS*, **247**, 48
 Kroupa, P. 2001, *MNRAS*, **322**, 231
 Lada, C. J., & Lada, E. A. 2003, *ARA&A*, **41**, 57
 Limongi, M., & Chieffi, A. 2018, *ApJS*, **237**, 13
 Loeb, A., & Rasio, F. A. 1994, *ApJ*, **432**, 52
 Lützgendorf, N., Baumgardt, H., & Kruijssen, J. M. D. 2013, *A&A*, **558**, A117
 MacLeod, M., Trenti, M., & Ramirez-Ruiz, E. 2016, *ApJ*, **819**, 70
 Madau, P., & Rees, M. J. 2001, *ApJL*, **551**, L27
 Mapelli, M. 2016, *MNRAS*, **459**, 3432
 Mapelli, M., Spera, M., Montanari, E., et al. 2020, *ApJ*, **888**, 76
 Marchant, P., Renzo, M., Farmer, R., et al. 2019, *ApJ*, **882**, 36
 McKernan, B., Ford, K. E. S., Lyra, W., & Perets, H. B. 2012, *MNRAS*, **425**, 460
 Miller, M. C., & Hamilton, D. P. 2002, *MNRAS*, **330**, 232
 Milone, A. P., Piotto, G., Bedin, L. R., et al. 2012, *A&A*, **540**, A16
 Moe, M., & Di Stefano, R. 2017, *ApJS*, **230**, 15
 Morscher, M., Pattabiraman, B., Rodriguez, C., Rasio, F. A., & Umbreit, S. 2015, *ApJ*, **800**, 9
 Ober, W. W., El Eid, M. F., & Fricke, K. J. 1983, *A&A*, **119**, 61
 Pattabiraman, B., Umbreit, S., Liao, W.-k., et al. 2013, *ApJS*, **204**, 15
 Portegies Zwart, S. F., Baumgardt, H., Hut, P., Makino, J., & McMillan, S. L. W. 2004, *Natur*, **428**, 724
 Portegies Zwart, S. F., McMillan, S. L. W., & Gieles, M. 2010, *ARA&A*, **48**, 431
 Renzo, M., Farmer, R. J., Justham, S., et al. 2020, *MNRAS*, **493**, 4333
 Rizzuto, F. P., Naab, T., Spurzem, R., et al. 2020, arXiv:2008.09571
 Rodriguez, C. L., Amaro-Seoane, P., Chatterjee, S., et al. 2018, *PhRvD*, **98**, 123005
 Rodriguez, C. L., Zevin, M., Amaro-Seoane, P., et al. 2019, *PhRvD*, **100**, 043027
 Roupas, Z., & Kazanas, D. 2019, *A&A*, **632**, L8
 Sana, H., de Mink, S. E., de Koter, A., et al. 2012, *Sci*, **337**, 444
 Sana, H., Gosset, E., & Evans, C. J. 2009, *MNRAS*, **400**, 1479
 Sigurdsson, S., & Hernquist, L. 1993, *Natur*, **364**, 423
 Spera, M., & Mapelli, M. 2017, *MNRAS*, **470**, 4739
 Spera, M., Mapelli, M., Giacobbo, N., et al. 2019, *MNRAS*, **485**, 889
 Stevenson, S., Sampson, M., Powell, J., et al. 2019, *ApJ*, **882**, 121
 Takahashi, K., Yoshida, T., & Umeda, H. 2018, *ApJ*, **857**, 111
 The LIGO Scientific Collaboration, the Virgo Collaboration, Abbott, R., et al. 2020a, arXiv:2010.14529
 The LIGO Scientific Collaboration, the Virgo Collaboration, Abbott, R., et al. 2020b, arXiv:2010.14550
 The LIGO Scientific Collaboration, the Virgo Collaboration, Abbott, R., et al. 2020c, arXiv:2010.14533
 Woosley, S. E. 2017, *ApJ*, **836**, 244
 Woosley, S. E. 2019, *ApJ*, **878**, 49
 Woosley, S. E., Blinnikov, S., & Heger, A. 2007, *Natur*, **450**, 390
 Zwart, S. F., Baumgardt, H., Hut, P., Makino, J., & McMillan, S. L. W. 2004, *Natur*, **428**, 724